Internal-Node Waveform Analysis of MMIC Power Amplifiers

Ce-Jun Wei, *Member, IEEE*, Yevgeniy A. Tkachenko, James C. M. Hwang, *Fellow, IEEE*, Kenneth R. Smith, and Andrew H. Peake

***Abstract*—A novel internal-node waveform probing technique has been demonstrated on a C-band monolithic microwave integrated circuit (MMIC) power amplifier. The error of the measurement and its perturbance to circuit operation was estimated and verified to be within ±10%. Valuable insight was obtained from the variation of waveforms as a function of frequency, drive and location. The potential impact of this technique includes MMIC design verification, in-situ device model extraction, process diagnosis, and reliability assessment.**

I. Introduction

NONINVASIVE, INTERNAL-NODE waveform probing is a valuable technique for diagnosis of digital and analog integrated circuits under real operating conditions. However, its application to monolithic microwave integrated circuits (MMIC's) has been limited by the accuracy of sampling oscilloscopes and the tendency for the probe to perturb the MMIC operation. The sampling oscilloscope generates only time-domain information, which makes it difficult to correct for instrument dispersion by standard frequency-domain calibration techniques. The typical microwave probe presents a major leakage path to the transmission line under test, because both the probe and the transmission line have characteristic impedances around 50 Ω.

Recently, with the availability of a microwave transition analyzer from Hewlett-Packard Co. and a high-impedance microwave probe from Cascade Microtech, Inc., we developed a novel internal-node waveform probing technique [1]. The transition analyzer generates information in both time domain and frequency domain. It uses a harmonic sampling technique to measure both the magnitude and phase of the harmonic components of a microwave signal. Knowing the harmonics, the voltage waveform can be reconstructed in time domain. Knowing the voltage waveforms at two different locations on a transmission line, the current waveform can be calculated.

As illustrated schematically in Fig. 1, the high-impedance probe has a series resistor at the probe tip which is followed by a standard 50 Ω transmission line. This series resistor acts as a potential divider to attenuate the signal, say, by a factor of ten in the case of a 500 Ω probe. The signal attenuation is usually not a concern, because the transition analyzer has a dynamic range greater than 60 dB. The high impedance presented by the probe to the transmission line causes little perturbance to the MMIC under test. If necessary, higher impedance (e.g., 1000 Ω) probes can be used to decrease the perturbance at the expense of increased attenuation.

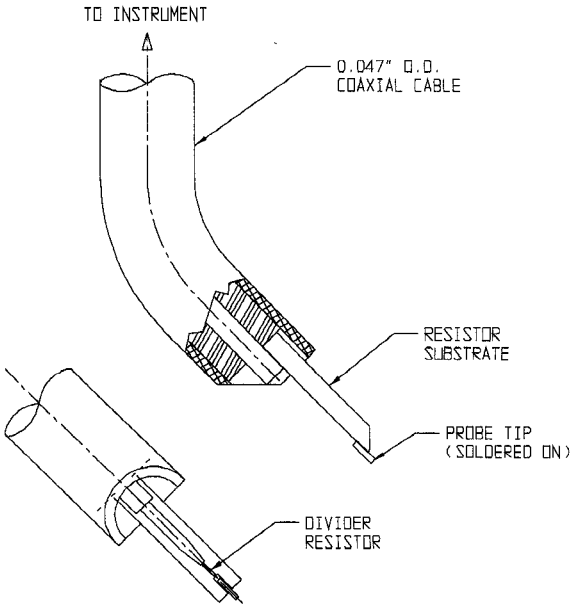

Fig. 1. Schematic illustration of the high-impedance probe. The probe tip is first connected to a series resistor (e.g., 450 Ω) then a 50 Ω coaxial line. The series resistor acts as a potential divider to attenuate the signal, say, by a factor of ten in the case of a 500 Ω probe. The signal attenuation is usually not a concern, because the 50 Ω coaxial line is, in turn, connected to a transition analyzer having a dynamic range greater than 60 dB. The high impedance presented by the probe to the transmission line causes little perturbance to the MMIC under test.

Using the novel technique, the voltage and current waveforms have been measured as a function of input frequency and power at various locations on a C-band MMIC power amplifier, without any layout modification or test structures [2]. The error of the measurement and its perturbance to circuit operation was estimated and verified to be less than ±10%. This paper expands on [2] by discussing the measurement set up and calibration procedure in detail. Actual data are presented to demonstrate the noninvasiveness, self-consistency, and reproducibility of the technique. Imbalance in signal distribution among the amplifier unit cells is quantified and its cause discussed. Load impedance and voltage stress as experienced by a transistor inside the MMIC is derived from the waveforms measured under both normal and overdrive conditions. Waveform-based device model extraction and verification is discussed elsewhere [3].

Manuscript received April 10, 1995; revised July 10, 1995.

C.-J. Wei, Y. A. Tkachenko, and J. C. M. Hwang are with Lehigh University, Bethlehem, PA 18015 USA.

K. R. Smith is with Cascade Microtech, Inc., Beaverton, OR 97005 USA.

A. H. Peake is with ITT GTC, Roanoke, VA 24019 USA.

IEEE Log Number 9415447.

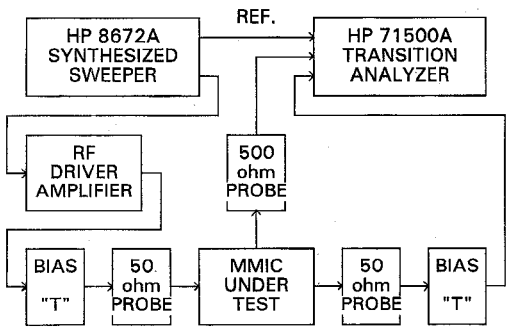

Fig. 2. Block diagram of the microwave waveform measurement set-up. The transition analyzer uses a harmonic sampling technique to measure both the magnitude and phase of the harmonic components of a microwave signal. The single tip, high impedance probe can be used anywhere on an MMIC to determine its internal voltage and current waveforms without disturbing the MMIC operation.

II. Measurement Technique

As illustrated in Fig. 2, the present measurement set up is similar to that described in [1], except for the 500 Ω probe. The newly developed Cascade Microtech FPM probe does not require ground contact, making it very convenient to probe anywhere on the MMIC. The new probe also has improved bandwidth, allowing up to the fifth harmonic of a 5 GHz signal to be reliably measured.

Before the new probe was used, various grounding arrangements, both on- and off-wafer, were evaluated experimentally. The results showed that, if the probe impedance and the measurement frequency is sufficiently high, the ground contact at the probe tip is not critical and, hence, can be omitted. The present probe has a single tip of 40 μm diameter which is ideal for probing 50 Ω microstrips on 100 μm thick GaAs. If necessary, the probe tip can be made smaller but it will not be as rugged.

To illustrate the noninvasive nature of the present probe, Fig. 3 shows the harmonic content of the output of an MMIC amplifier with the RF signal launched and measured through a pair of standard 50 Ω probes as illustrated in Fig. 2. A third, high-impedance probe was then brought in contact with different parts of the MMIC while its output was continuously measured. It can be seen that the fundamental output signal is not affected by the high- impedance probe whereas variations in higher harmonics are less than −40 dB of the fundamental.

The calibration procedure mainly involves characterization of frequency dispersion of the probe—an advantage for the present technique over conventional time-domain-based techniques. The calibration is performed on a microwave network analyzer, with a high-impedance probe and a standard 50 Ω probe contacting the two ends of a 50 Ω through line. The 50 Ω probe and the through line were previously calibrated using standard frequency-domain techniques. Therefore, they can be de-embedded from the measured S-parameters to arrive at the S-parameters of the high-impedance probe. Ideally, to properly account for the coupling capacitance between the high-impedance probe and the transmission line under test, the through line used in the calibration should have similar dimensions as the transmission line under test. However, this requirement can be relaxed when the probe tip is smaller than the transmission line width.

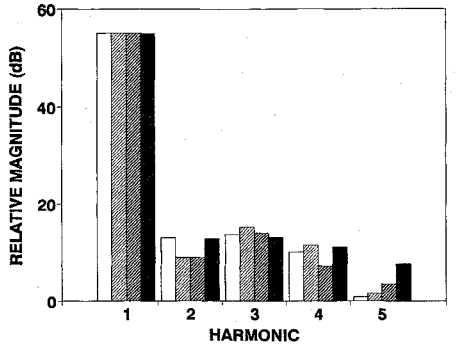

(a)

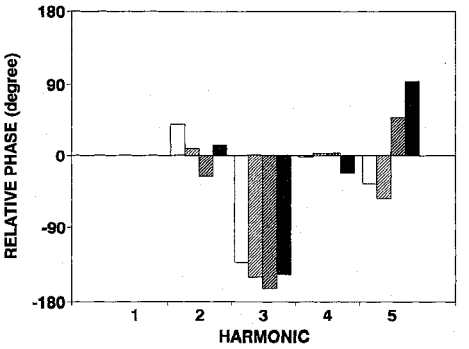

(b)

Fig. 3. Noninvasiveness of the present measurement technique. Harmonic (a) magnitudes and (b) phases are measured at the MMIC amplifier output with the high-impedance probe (□) lifted or contacting (□) drain node, (□) gate node, and (■) matching element of a MMIC unit cell. The input drive is 28 dBm at 5 GHz.

Fig. 4 shows the measured input impedance and insertion loss of a 500 Ω probe as a function of frequency. Due to the parasitic coupling capacitance, the input impedance gradually drops to 160 Ω at 26 GHz, at which frequency the perturbance to the MMIC under test can become significant. On the other hand, the resonances around 2 and 5 GHz are caused by omitting the ground contact of the probe, but can be readily calibrated out. This calibration is not critical if the fundamental frequency of measurement is above the resonant frequencies as in the present case. The insertion loss, being less than 20 dB, is not a concern due to the large dynamic range of the transition analyzer as mentioned in the beginning. After the probe and the associated connectors and cables are calibrated, the waveforms measured at the transition analyzer can be transformed to the very tip of the probe, where it intercepts the transmission line under test. Typically, the phases of all the harmonics are referenced to the MMIC amplifier output, which is simultaneously measured using the second input channel of the transition analyzer as indicated in Fig. 2.

To illustrate the reproducibility of the present technique, Fig. 5 shows the drain-gate voltage waveforms measured by two different probes from the unit cell of the same location on three different MMIC's. The difference between the *same* unit cell of *different* MMIC's is found to be smaller than the difference between *different* unit cells of the *same* MMIC, which underscores the reproducibility of both the MMIC fabrication and testing techniques. The dynamic range

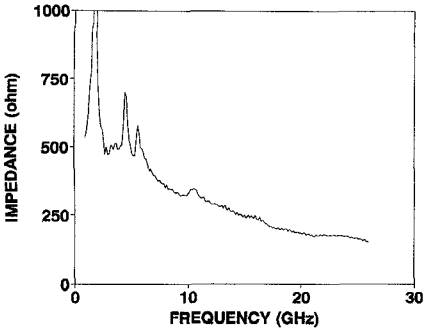

(a)

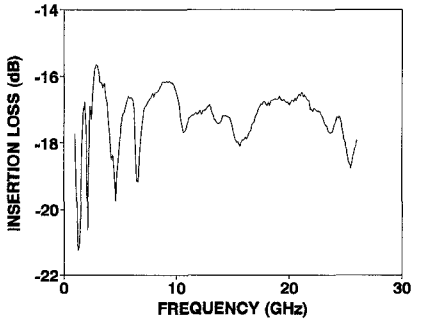

(b)

Fig. 4. Bandwidth of a high-impedance probe. (a) Input impedance and (b) insertion loss of a probe having a nominal value of 500 Ω was measured as a function of frequency. Once measured, the frequency dispersion can be readily calibrated for the present frequency-domain technique. The parasitic coupling capacitance causes the probe impedance to drop to 160 Ω at 26 GHz, at which frequency the perturbance to the MMIC under test can be significant. The insertion loss, being approximately −18 dB, is caused by the potential divider and other discontinuities and loss mechanisms.

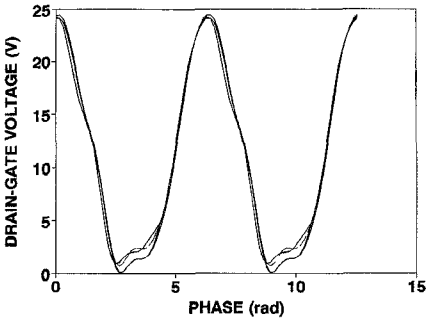

Fig. 5. Dynamic range and reproducibility of the present technique. The drain-gate voltage waveforms were measured by two different probes having (—) 500 and (···) 1000 Ω impedances, respectively, from the unit cell of the same location on three different MMIC's. The input drive is 33 dBm at 5 GHz.

achieved by the present measurement technique encompasses the voltage range of typical MMIC's.

From the voltage waveforms measured at two different locations on a transmission line, the current waveform can be calculated as in the following. Giving the Nth harmonic voltages measured at two adjacent locations, V_N and V_N', the incident and reflected harmonic voltage waves, A_N and B_N, can be calculated according to

$$A_N = \{V_N \exp(jN\omega\tau) - V_N'\}/2\sin(N\omega\tau) \quad (1)$$

$$B_N = -\{V_N \exp(-jN_{\omega\tau}) - V_N'\}/2\sin(N\omega\tau) \quad (2)$$

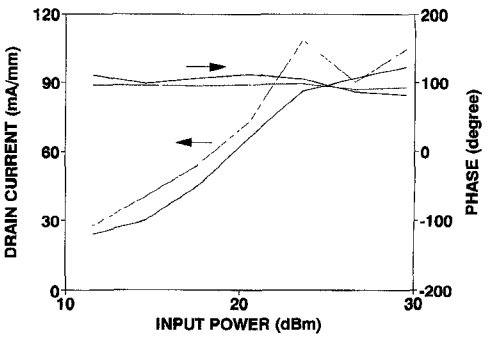

Fig. 6. Self-consistency of current waveform measurement across a transmission-line "T"-junction. The current measured on the main line is compared to the sum of the currents measured on the two branch lines, as a function of input power at 5 GHz. Notice that the currents track each other in both magnitude and phase. (—) main line. (···) sum of branches.

TABLE I
WORST-CASE ERROR ANALYSIS

Source of Error	Magnitude Error	Phase error
Transition Analyzer	±10%	±7°
Probe Calibration	±1%	±3°
Probe Positioning	<1%	<1°

where $j = \sqrt{-1}$; ω is the angular frequency; τ is the time it takes for the wave to propagate between the two locations. The harmonic current, I_N, is then evaluated by

$$I_N = (A_N - B_N)/Z_0 \quad (3)$$

where Z_0 is the characteristic impedance of the transmission line under test. Ideally, the distance between the two locations should be chosen so that the phase delay for the highest harmonic of interest is close to, but not greater than 180°.

A self-consistency test involves the branch currents at a transmission line "T" junction. Fig. 6 shows that, when the measured branch currents are added together, they are within ±10% of that measured on the main line, in terms of both magnitude and phase.

With carefully designed calibration and test procedures, the accuracy of the present technique appears to be limited by the error of the transition analyzer. Table I lists the worst-case estimate of major error sources. Theoretically, the worst case error can be ±11% in magnitude and ±10° in phase. In practice, the error is usually much smaller than the worst case estimate. This is especially true with signal averaging in CW measurements.

The results presented in the following were measured on a C-band, single-stage, 5 W, MMIC amplifier. The MMIC amplifier contains four MESFET unit cells. Each MESFET unit cell comprises twenty gate fingers. Each gate finger is 0.5 μm long and 175 μm wide. The typical drain and gate biases are 9 and −2 V, respectively.

III. RESULTS AND DISCUSSION

Fig. 7 shows the power performance of the MMIC amplifier at 5 GHz. Similar performance was obtained from 4 to 6 GHz, with somewhat lower output power at 4 or 6 GHz. Fig. 8 illustrates the unit-cell drain and gate voltages at 5.375

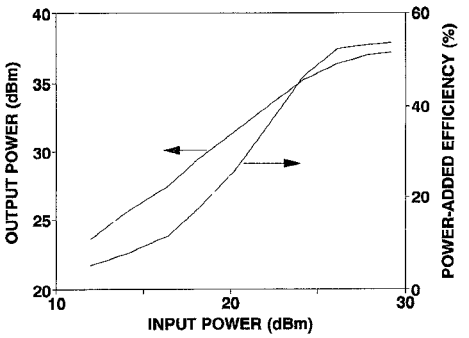

Fig. 7. Power performance of the MMIC amplifier at 5 GHz. Input powers of 26, 28, and 33 dBm correspond to gain compressions of 1, 3, and 8 dB, respectively.

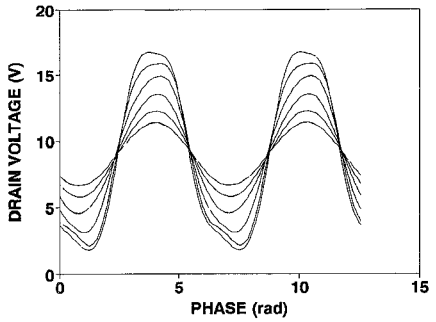

(a)

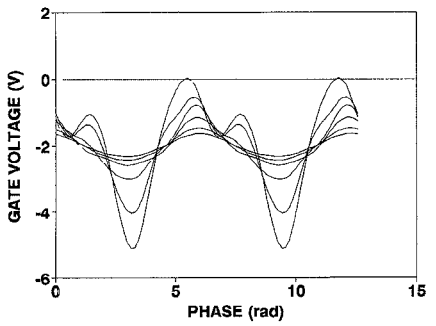

(b)

Fig. 8. Unit-cell (a) drain-voltage and (b) gate-voltage waveforms at 5.375 GHz with input powers of 14, 17, 20, 23, 26, and 28 dBm. Under linear drive levels, the drain voltage lags the gate voltage by approximately 1 rad. Once the drive exceeds 26 dBm, both waveforms are greatly distorted and their phase relationship becomes ambiguous.

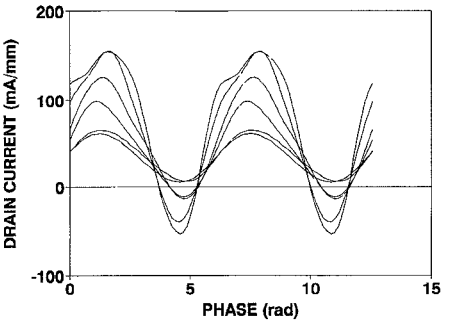

(a)

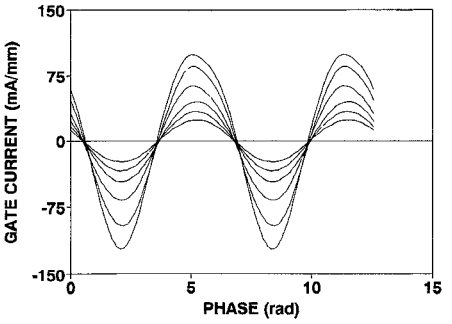

(b)

Fig. 9. Unit-cell (a) drain-current and (b) gate-current waveforms at 5.375 GHz with input powers of 14, 17, 20, 23, 26, and 28 dBm.

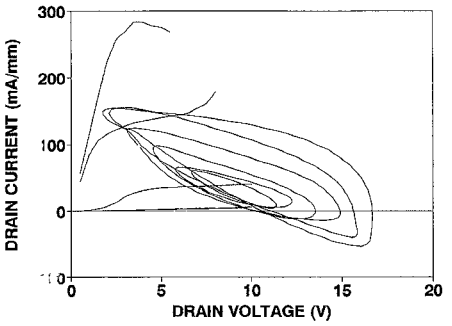

Fig. 10. Dynamic load contours of a unit cell superimposed on its dc drain characteristics. High-impedance output match is used to achieve high power-added efficiency at the expense of saturated output power. The associated large voltage swing can be a reliability concern. The load contours are constructed from the voltage and current waveforms of Figs. 8 and 9. The dc characteristics are measured under a gate bias of 0, −1, and −2 V.

GHz under different input drive levels. The voltages were measured on the unit-cell input and output lines, after all twenty fingers are interconnected and before any matching element is branched on. It can be seen that, under linear drive levels, the drain voltage lags the gate voltage by approximately 1 rad. Once the drive exceeds 26 dBm, corresponding to approximately 1 dB gain compression, both drain and gate voltages are greatly distorted and their phase relationship becomes ambiguous.

From the voltage waveforms measured at different locations along each branch line, the total unit-cell drain and gate currents can be determined as shown in Fig. 9. From the measured drain current and voltage waveforms, the dynamic load contours can be plotted as in Fig. 10. Fig. 10 includes also dc drain characteristics as references. Conventional output impedance matching would have the load contour intercept the knee of the dc drain current curve, in order to maximize the saturated output power. It can be seen in Fig. 10 that a relatively high matching impedance was used to allow the load contour to swing below the knee, thereby achieving higher power-added efficiency but lower saturated output power. Such a high-impedance match also causes the drain voltage to swing higher which, together with a large gate- voltage swing, may exceed the threshold voltage for gate-drain breakdown and hot-electron-induced degradation [4].

Fig. 11 shows that the peak drain-gate voltage measured with an input drive of 28 dBm can exceed 22 V at certain frequencies. Such a peak voltage may cause gate-drain breakdown of the MESFET. Therefore, conventional wisdom

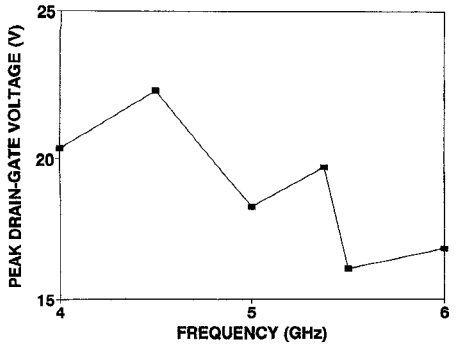

Fig. 11. Peak drain-gate voltages from 4 to 6 GHz, calculated from the drain- and gate-voltage waveforms measured at each input frequency. Although the drain bias is only 9 V and the gate bias −2 V, under an input power of 28 dBm, the peak drain-gate voltage can exceed 22 V at certain frequencies.

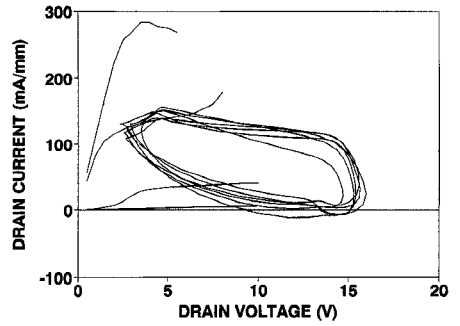

Fig. 12. Dynamic load contours of another unit cell under RF overdrive conditions. The bias and input conditions are the same as in Fig. 10 except that the input power is increased to 28, 29, 30, ... 33 dBm. At 28 dBm, the load contour is very similar to that of the MMIC of Fig. 10, which underscores the reproducibility of both the MMIC fabrication and testing techniques. When the input power is greater than 28 dBm, the drain voltage is clamped at 16 V but the drain-gate voltage can continue to increase due to increased gate voltage swings.

of biasing the drain at half of its dc breakdown voltage (measured with the gate voltage at pinch-off) may not be adequate to protect it from degradation. Further, using the present waveform probing technique, we were able to quantify the deep breakdown characteristics where dc measurement would cause the MESFET to burn out. The waveform results indicate that RF breakdown characteristics may or may not agree with that extrapolated from the dc characteristics [5].

To assess the electrical stresses experienced by a unit cell under RF overdrive conditions, another MMIC amplifier was driven at 5 GHz with an input power as high as 33 dBm, or 8 dB in compression. Under such a large electrical stress, long-term gradual degradation under normal operations can often be accelerated to within a few hours. Fig. 12 shows the dynamic load contours under such conditions. It can be seen that the drain voltage is clamped at 16 V. However, the peak drain-gate voltage continues to increase with increasing input power due to increased gate-voltage swings. The load contour at 28 dBm for this MMIC is similar to that for the MMIC shown in Fig. 10, confirming again the reproducibility of both the MMIC fabrication and testing techniques.

Next, the drain bias of the present MMIC amplifier is stepped up from 8 to 14 V, with the gate bias and the input power held at −2 V and 33 dBm, respectively. Fig. 13 shows that the peak drain-gate voltage increases approximately

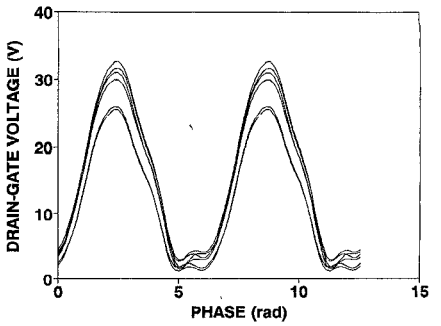

Fig. 13. Unit-cell drain-gate voltage waveforms under simultaneous dc and RF stresses. Drain bias = 8, 10, 11, 12, 13, and 14 V. Gate bias = −2 V. Input drive = 33 dBm at 5 GHz. The peak drain-gate voltage increases approximately linearly with the drain bias. However, this increase is due primarily to the increased negative swing of the gate voltage.

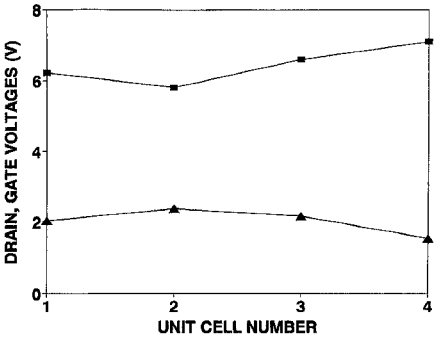

Fig. 14. Variation of fundamental (■) drain and (▲) gate voltages across the four unit cells of the MMIC amplifier. The inner cells appear to have higher input level (probably due to shorter input path) but lower gain (probably due to higher temperature) than the outer unit cells. These two effects compensate each other to even out the output level. Input = 28 dBm at 5 GHz.

linearly with the drain bias. From the detailed waveforms, this increase is also due primarily to the increased negative swing of the gate voltage.

Due to circuit interactions or processing and heat-sinking variations, internal voltages can vary from unit cell to unit cell in addition to being a function of input frequency and power. Fig. 14 shows the fundamental magnitude of the drain and gate voltages measured on each unit cell of the MMIC amplifier. It can be seen that the variation in drain voltage is comparable to the measurement error, whereas significant variation in gate voltage exists between inner and outer unit cells. The inner cells appear to have higher input level (probably due to shorter input path) but lower gain (probably due to higher temperature) than the outer unit cells. These two effects compensate each other to even out the output level. Fig. 15 shows that higher harmonics have also been uniformly suppressed to below −15 dB of the fundamental.

To verify the circuit design, the circuit impedance experienced by a unit cell can be calculated from the measured waveforms. Fig. 16 shows the fundamental load impedance as experienced by a unit cell from 4 to 6 GHz. It can be seen that the load impedance is rather constant from 4.5 to 5.5 GHz. The load resistance is higher at both 4 and 6 GHz, while the load reactance is lower at 4 GHz but higher at 6 GHz. The resulted mismatches at 4 and 6 GHz may explain the measured output roll-off at these frequencies. However, in spite of the

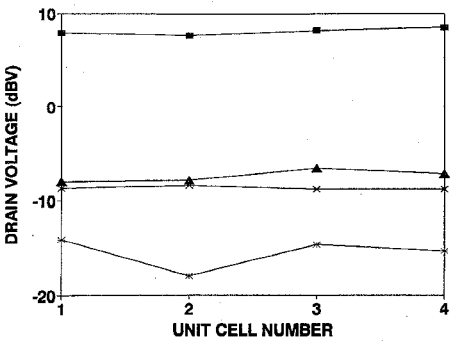

Fig. 15. Harmonic analysis of the drain voltage across the same four unit cells of Fig. 13. Higher harmonics have been uniformly suppressed to below −15 dB of the fundamental. (■) fundamental, (▲) second, (×) third, and (∗) fourth harmonics.

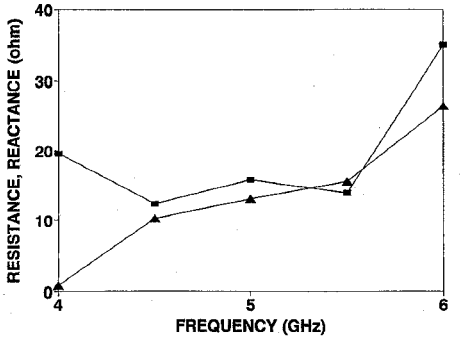

Fig. 16. Fundamental load (■) resistance and (▲) reactance as experienced by a unit cell from 4 to 6 GHz. The load impedance is rather constant from 4.5 to 5.5 GHz. The variations of the load impedance at 4 and 6 GHz resulted in output power roll off at these frequencies.

variations, the load reactance is always inductive which is needed for conjugate match to the unit cell output reactance, the latter being always capacitive.

IV. Conclusion

In conclusion, an MMIC internal-node waveform probing technique has been developed and demonstrated. Valuable insight was obtained from the variation of waveforms as a function of frequency, drive and location. The peak swing of the MESFET drain- gate voltage under different drive conditions was quantified, which information can be used to predict the MMIC lifetime against gradual degradation under RF overdrive. Variation of unit-cell characteristics within an MMIC was observed and attributed to differences in RF-input and heat-dissipation paths. The load impedance actually experienced by the MESFET within an MMIC was verified to be optimum for the maximum power-added efficiency at somewhat lower saturated output power. These examples illustrate the potential for the present technique to impact broadly on MMIC design verification, process control and reliability assessment.

References

[1] C. J. Wei, Y. A. Tkachenko, and J. C. M. Hwang, "Noninvasive waveform probing for nonlinear network analysis," in *IEEE MTT-S Int. Microwave Symp. Dig.*, May 1993, pp. 1347–1350.

[2] C. J. Wei, Y. A. Tkachenko, J. C. M. Hwang, K. R. Smith, and A. H. Peake, "Internal-node waveform probing of MMIC power amplifiers," in *IEEE Microwave and Millimeter-Wave Monolithic Circuits Symp. Dig.*, May 1995, pp. 127–130.

[3] C. J. Wei, Y. E. Lan, J. C. M. Hwang, W. J. Ho, and J. A. Higgins, "Waveform modeling and characterization of microwave power heterojunction bipolar transistors," in *IEEE MTT-S Int. Microwave Symp. Dig.*, May 1995, pp. 1239–1242.

[4] Y. A. Tkachenko, Y. Lan, D. S. Whitefield, C. J. Wei, J. C. M. Hwang, T. D. Harris, R. D. Grober, D. M. Hwang, L. Aucoin, and S. Shanfield, "Hot-electron-induced degradation of metal-semiconductor field-effect transistors," in *Tech. Dig. IEEE GaAs IC Symp.*, Oct. 1994, pp. 259–262.

[5] Y. A. Tkachenko, J. W. Bao, C. J. Wei, and J. C. M. Hwang, "Waveform analysis of GaAs FET breakdown," in *Automated RF Techniques Group Conf. Dig.*, May, 1995, pp. 139–142.

Ce-Jun Wei, (M'93) for a photograph and biography, see this issue p. 2903.

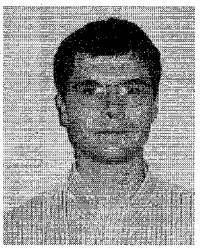

Yevgeniy A. Tkachenko was born in Kiev, Ukraine, in 1968. He received the electrical engineer's degree from Kiev Polytechnical Institute in 1993 and the B.S., M.S., and Ph.D. degrees in electrical engineering from Lehigh University in 1991, 1993, and 1995, respectively.

Since 1991, he has been working on characterization, modeling, and reliability of microwave devices and circuits at Lehigh's Compound Semiconductor Technology Laboratory. In June 1995, he joined Alpha Industries Inc., Woburn, MA, as Senior Engineer.

James C. M. Hwang, (M'81–SM'82–F'94) for a photograph and biography, see this issue p. 2903.

Kenneth R. Smith received the B.S. in general engineering from Oregon State University in 1979.

He worked at Tektronix where he developed multilayer thin-film processes and multichip packages, and managed hybrid circuits research and development, until he became Hybrid Circuits Division Manufacturing Manager. He then worked as Director of Operations at Cogent Research, a parallel processing computer startup. Four years ago, he joined Cascaded Microtech where he applied Cascade's high-frequency capabilities to developing tours for IC package, microwave hybrid, and multichip module characterization. Most recently he led a team to develop a membrane probe capable of probing IC's with up to 36 lines and 20 GHz bandwidth. He is currently Vice President and Membrane Probe Manager at Cascade. He has published over twenty papers and been granted eight patents.

Andrew H. Peake received a B.Sc. (Honors) in physics and physical electronics from the University of Bath, England, in 1978.

From 1978 to 1982, he worked as Process Development Scientist for Plessey Research (Caswell) helping to develop ion implantation for GaAs FET's and 0.3 μm gate length Q-band devices. In 1982 he joined Raytheon SMDO, where he developed GaAs FET's for Ku-K band amplifiers. He later became the Wafer Processing Manager for discrete devices at SMDO. In 1988 he transitioned back into device design developing PHEMT devices for commercial applications. His additional tasks included reliability evaluation of GaAs FET's. In 1991 he joined ITT's Gallium Arsenide Technology Center, where he is currently a Principal Member of Technical Staff and the Quality Manager. He has authored several papers on thermal design and high frequency GaAs FET's.